NASA TECHNICAL MEMORANDUM 107570

MEASUREMENT OF MULTIAXIAL PLY STRENGTH BY AN OFF-AXIS FLEXURE TEST

John H. Crews, Jr. and Rajiv A. Naik

March 1992

Presented at the ASTM 11th Symposium on Composite Materials: Testing and Design; Pittsburgh, PA; May 4-5, 1992

National Aeronautics and
Space Administration

Langley Research Center
Hampton, Virginia 23665

ABSTRACT

An off-axis flexure (OAF) test has been presented to measure ply strength under multiaxial stress states. This test involves unidirectional off-axis specimens loaded in bending, using an apparatus that allows these anisotropic specimens to twist as well as flex without the complications of a resisting torque. A 3D finite element stress analysis verified that simple beam theory could be used to compute the specimen bending stresses at failure. Unidirectional graphite/epoxy specimens with fiber angles ranging from 90° to 15° have combined normal and shear stresses on their failure planes that are typical of 45° plies in structural laminates. Tests for a range of stress states with AS4/3501-6 specimens showed that both normal and shear stresses on the failure plane influenced cracking resistance. This OAF test may prove to be useful for generating data needed to predict ply cracking in composite structures and may also provide an approach for studying fiber-matrix interface failures under stress states typical of structures.

Keywords.- composite, ply strength, test, multiaxial, off-axis flexure

INTRODUCTION

Ply cracks are usually the first damage to develop when composite laminates are loaded to failure. In structural applications, these cracks often develop under multiaxial stress states involving a tension normal stress acting perpendicular to the fiber direction and a shear stress parallel to the fibers. Therefore, ply strength data should include the combined effects of these two stresses. However, very little testing has been done to measure ply cracking resistance under multiaxial loading because of difficulties with current test methods.

Two general approaches have been used in the past to measure multiaxial ply strength. The first approach uses tensile specimens with an off-axis fiber orientation, for example see [1] or [2]. Cracks initiate on the off-axis plane, which is subjected to both normal stress and longitudinal shear stress, and then grow in the fiber direction. The ratio of the normal stress to the shear stress can be varied by using different fiber angles. Unfortunately, however, anisotropy of the off-axis specimen causes shear strains to develop when the tensile strains are applied. Typically, the specimen grips constrain this shear strain and thereby introduce undesirable stress concentrations which lead to premature failures at or near the grip. Although, numerous gripping and tabbing concepts have been used to reduce these stress concentrations [3-7], none of them completely eliminates this problem.

In the second approach, tubular specimens with fibers wound in the hoop direction are loaded in an axial/torsion test machine that simultaneously applies an axial tension and a torque, for example see [8]. The ratio of these loads determines the ratio of normal stress to shear stresses for the failure plane. This test produces the desired range of stress states for multiaxial strength measurements but requires expensive specimens and a rather complex test machine. Furthermore, tubular specimens are also subject to stress concentrations caused by gripping [9-10] and, therefore, require special end tabs to reduce this problem.

The objective of the present paper is to present a simple test to measure multiaxial ply strength. This test involves unidirectional off-axis specimens loaded in bending, using an apparatus that allows these anisotropic specimens to twist as well as flex without a resisting torque. After, the testing concept is described, the off-axis flexure test apparatus is presented. A 3-D finite-element stress analysis is then used to evaluate

the test concept and to evaluate the proposed data reduction procedure for calculating the multiaxial stresses on the failure plane. The off-axis flexure test is demonstrated and discussed using AS4/3501-6 graphite/epoxy specimens with a 24-ply unidirectional layup.

NOMENCLATURE

b	specimen width
d	specimen thickness
L	distance between specimen supports
P	applied load
w	z-direction displacement
x,y,z	Cartesian coordinates
α	specimen fiber angle
σ_{12}	shear stress in fiber direction
σ_{22}	normal stress perpendicular to fibers
σ_{xb}	beam theory bending stress
σ_{xx}	normal stress in x-direction
σ_{xy}	shear stress in xy-plane
σ_{yy}	normal stress in y-direction
σ_{zz}	normal stress in z-direction

SPECIMEN CONFIGURATION AND TEST PROCEDURE

As mentioned, the present approach involves testing off-axis specimens in bending to produce ply cracking failures under multiaxial stress states. Although similar off-axis specimens have been tested previously in uniaxial tension, they have not been tested in flexure. The off-axis flexure (OAF) test apparatus was developed to exploit the simplicity of the off-axis specimen while avoiding the problems associated with gripping this specimen. The specimen and test apparatus are described in this section.

Specimen Configuration and Loading

Figure 1(a) shows the plan view of the off-axis specimen. Specimens were cut from a 24-ply unidirectional laminate made with AS4/3501-6 graphite/epoxy. Each specimen orientation was indicated by the fiber angle α, as shown in figure 1(a). The fiber angles of 90°, 75°, 60°, 45°, 30°, and 15° were used. Figure 1(b) shows the edge view of the specimen and the applied load (P). For the 24-ply laminate used in this study, specimen thickness (d) was nominally 3.18 mm. Specimen width (b) was 6.35 mm and its length was 53.3 mm.

For the loading shown in figure 1(b), tensile failure is expected to initiate on the lower surface at the midspan of the specimen and then to propagate in the fiber direction. The axial bending stress (σ_{xx}) produces a multiaxial stress state on the failure plane. When referenced to the material principal axes, this stress state can be represented by σ_{22}, the normal stress transverse to the fiber, and σ_{12}, the longitudinal shear stress in the fiber direction.

Off-Axis Flexure Test Apparatus

As previously mentioned, because of anisotropy, the off-axis specimen develops twist as well as flexure as it deforms under the applied three-point bending loads. Figure 2(a) schematically illustrates this deformation with twist at each end of the specimen. If the ends of the specimen are clamped to prevent this twist, the resulting torque on the specimen would produce a non-uniform shear stress distribution that would seriously complicate strength measurements. If simple end supports are used, the twist will cause one side of the specimen to lift off the support and a "point-load" reaction would develop at the opposite side of the specimen. Such eccentric loading would also apply an undesirable torque on the specimen.

The concept used by the present apparatus is illustrated in figure 2(b). The specimen supports are attached to ball bearings that rotate freely to accommodate twist without introducing a torque reaction. The loading nose prevents rotation at the specimen midspan and thereby stabilizes the specimen. The twist is, therefore, equal and opposite at the two specimen supports. This approach allows an off-axis specimen to be loaded to failure under bending stresses which will be analyzed in the next section.

A photograph of the off-axis flexure apparatus is shown in figure 3. A one-piece steel base holds both ball bearings which were installed with a press fit. The specimen rests on steel supports (not visible in this photograph) having a 3.18 mm radius. These supports are bonded to spacers which are bonded to the inner race of each bearing. The steel loading nose also has a 3.18 mm radius. This three-point bending apparatus has a 40.6 mm span (L), which allowed the specimen to overhang each support by 6.35 mm. An end-view photograph of the apparatus is shown in figure 4. This figure

shows the specimen supports and the spacers that center the specimen cross-section on the axis of rotation for the two ball bearings. The specimen twist is evidenced by the opposite rotations of these supports. The end of this 15^{o} specimen, which is loaded to about 80% of failure, was painted gray to make its twist more visible in this photograph.

The OAF specimens were loaded to failure using a screw-driven test machine with a displacement rate of 0.51 mm/min. As previously mentioned, all specimens were cut from the same 24-ply unidirectional laminate which was made using a caul plate. To avoid differences that might exist between the two sides of the laminate, all specimens were tested with the caul plate side as the bottom surface.

STRESS ANALYSIS

The 3D finite element stress analysis was conducted to evaluate the OAF specimen and to evaluate the use of simple beam theory to calculate the failure stresses in this specimen. The stress analysis focused on the bottom surface of the specimen at its midspan, the expected failure initiation site. The 3D finite element model is shown in figure 5. This model consisted of eight-noded isoparametric elements, with mesh refinement near the midspan and near the load reaction regions. The model dimensions are expressed in terms of its depth d. Its width b is equal to 2d and span is 16d, with a support overhang of 2.5d at each end. Although the 16d span is larger than the actual 12d value for the specimens tested, this discrepancy was not believed to be important, because both values are sufficiently large for simple beam theory to apply.

The following elastic properties were used to represent unidirectional AS4/3501-6 graphite/epoxy [11]:

$$E_{11} = 144.8 \text{ GPa} \qquad E_{22} = E_{33} = 9.65 \text{ GPa}$$

$G_{12} = G_{13} = 5.86$ GPa $\qquad G_{23} = 3.71$ GPa

$\nu_{12} = \nu_{13} = \nu_{23} = 0.30$

The corresponding model properties were calculated by transforming these unidirectional properties through the specimen fiber angle. This 3D stress analysis was conducted using the MSC NASTRAN finite element code.

The midspan load was introduced by applying a uniform w (z-direction) displacement at the top surface, simulating loading nose contact. Specimen contact with the rotatable supports was simulated using two constraints: 1) the middle support node (x=+/-8d, y=0, z=d/2) was fixed to prevent y- and z-displacement and 2) z-displacements for the other support nodes were constrained to lie on a straight line which could rotate about the middle node. The reaction loads were summed to determine the applied load P.

The finite element analyses were conducted for three cases: specimens with off-axis fiber angles of 75°, 45°, and 15°. To facilitate comparisons, the finite element stresses for each case were normalized by the maximum beam theory stress, σ_{xb}, calculated using

$$\sigma_{xb} = 3PL / 2bd^2 \qquad (1)$$

Results for the $\alpha = 75^{\circ}$ case are presented in figure 6 as stress distributions across the specimen width at its midspan (x=0). The symbols in this figure represent finite element results and the solid curves are fits to these results. Horizontal lines indicate the reference levels of 0 and 1 for the stress scale. The uniform displacement imposed on the top of the specimen produced the loading nose contact stress σ_{zz}(open circular symbols). This σ_{zz} distribution is nonuniform because of anticlastic curvature of the specimen at its midspan. The symmetry of this σ_{zz} distribution shows that the specimen did not twist at its midspan. The σ_{xx} bending stresses (solid circular symbols) are essentially uniform across the lower surface of the specimen. The σ_{yy} and σ_{xy} stresses (triangle and

square symbols, respectively) at the bottom of the specimen are negligibly small, indicating the desired uniaxial stress state in the failure initiation region. Because the σ_{xx} average across the width and the beam theory value differ only by about two percent, failure of the 75° off-axis flexure specimen can be analyzed using beam theory with negligibly small errors.

Figure 7 shows stress distributions for the $\alpha = 45^{\circ}$ case. The σ_{zz} contact stresses are more nonuniform than in the previous case and are zero near the edges. Two nodes closest to each edge were released to allow separation between the specimen and the loading nose. However, despite this separation, the σ_{xx} stress is nearly uniform, and the σ_{xy} and σ_{yy} are very small. The σ_{xx} values near the center of the specimen agree almost exactly with beam theory and the σ_{xx} average agrees within two percent. These results show that beam theory can also be used to calculate accurate σ_{xx} values for a 45° specimen.

Figure 8 shows that the σ_{zz} stress distribution for the 15° case is similar to the 45° case. Although the σ_{xy} and σ_{yy} stresses are again negligible, the σ_{xx} variation is larger than the variation in the other two cases. However,its average is within one-half percent of the beam theory and, except very near the edges, the σ_{xx} values are within about five percent of the beam theory level. This discrepancy was considered to be marginally acceptably for the present study. This σ_{xx} comparison suggests that 15° is near the limiting fiber angle for the present specimen configuration.

These stress results show that the rotatable supports allowed the OAF specimen to twist without introducing an undesirable torque reaction. As a result, OAF test data can be analyzed using simple beam theory. For each test, the σ_{xb} can computed using the measured failure load in equation (1).

The corresponding σ_{12} and σ_{22} stresses on the failure plane can then be calculated using

$$\sigma_{12} = \sigma_{xb} \sin(\alpha) \cos(\alpha) \tag{2}$$

and

$$\sigma_{22} = \sigma_{xb} \sin^2(\alpha) \tag{3}$$

TEST RESULTS AND DISCUSSION

Typical load displacement curves are shown in figure 9 for each specimen angle. In all tests, the specimens failed unstably by cracking from the bottom surface at or very near the specimen midspan, as expected. The crack formed perpendicular to the bottom surface and grew in the fiber direction across the specimen width. The largest displacement at failure (about 1.3 mm) was only about 40% of the specimen thickness. Therefore, the flexural response of the OAF specimen was within the range of linear beam theory. However, the slight nonlinearity in the curves for α values of 15° and 30° suggests that some matrix yielding occurred before failure in these cases. Although matrix yielding was not included in this initial evaluation of the OAF test, it may be important and should be considered in a future study.

The σ_{22} and σ_{12} stresses at failure are presented in table 1 and plotted against one another in figure 10. The slopes of the dashed lines in this figure indicate the σ_{22}/σ_{12} stress ratio for each α value and range from ∞ for the 90° case to 0.27 for the 15° case. The symbols in figure 10 represent an average of five tests for each fiber angle and the brackets indicate the data range for each case. The solid curve is a fit to the average values. For fiber angles between 90° and 45°, the failures appear to be governed by σ_{22}, because the magnitude of σ_{12} appears to have very little influence on cracking resistance in this range. In fact, there is a

slight increase in σ_{22} for the 75° case compared to the 90° case; similar trends have been observed for delamination toughness under combined tension and shear loading [12]. For fiber angles smaller than 45°, figure 10 shows that shear loading has a noticeable effect. For example, the σ_{22} strength component for the 15° case is only about 40 percent of the 90° case.

Testing with fiber angles smaller than 15° may be possible, however, the applied bending stresses may be too nonuniform to be predicted accurately by beam theory, as mentioned earlier. Also, matrix yielding may become a serious stress analysis problem for smaller angles. Furthermore, for very small angles, either tensile fiber failure or upper surface compressive failure may occur before matrix cracking initiates on the off-axis plane.

The OAF test uses multiaxial stress states that are typical of ply stresses in laminates. For example, an OAF test with α of 30° has a σ_{22}/σ_{12} ratio like a 45° ply in a quasi-isotropic laminate with uniaxial loading. An α of 60° corresponds to a similar case with 2/1 biaxial loading on the laminate, and 30° corresponds to -2/1 loading. As a result, OAF tests could provide a suitable data base for prediction the onset of matrix cracking in laminated structures. In this context, the solid curve through the data in figure 10 could be viewed as a failure criterion for ply cracking resistance.

Although similar stress states can be produced with the off-axis tension test, the OAF test is believed to offer several important advantages. First, as previously mentioned, off-axis tension specimens have stress concentrations that cause premature failures near the grips where the stress state is complex. A second advantage is the small volume of material that is stressed to failure in an OAF test, compared to the off-axis tension test. In laminated structures, typical matrix cracks develop in single

plies and usually initiate first in rather small local regions, such as near fastener holes or edges. The OAF test approximates this "small local volume" condition better than the off-axis tension test which uses a rather long specimen under uniform stress. In reference 13, the transverse flexure test (the present 90^{o} case) and the transverse tension test were compared, and the flexure test was recommended for ply strength testing because of this volume consideration. The relatively small overall size of the OAF specimen provides an additional advantage, which could be especially important for studies of new materials and processes when only small quantities of material are available.

Because ply cracking often involves fiber-matrix interface cracks, the OAF test may also be useful in fiber-matrix interface studies. Reference 13 showed that the transverse flexure test (the present 90^{o} case) was sensitive to interface treatment and, therefore, useful for fiber-matrix interface studies. Reference 13 also found the short beam shear test to be a good indicator of interface treatment effects, but its results were significantly different from those measured by the transverse flexure test. Reference 13 suggested that tension and shear strengths of the fiber-matrix interface were governed by different failure mechanisms and, therefore, emphasized the need to evaluate interfaces under both types of loading. The OAF test inherently involves both tension and shear loading and has the highly desirable advantage of using stress states that are typical of composite plies. Therefore, the OAF test could provide interface optimization results that are relevant to typical structures.

Figure 11 shows a photomicrograph of a fracture surface for each of the six off-axis flexure cases. The photomicrographs were taken near the middle of the fracture surface at a location very close to the lower surface. This location was about 10 to 15 fiber spacings from the bottom of the specimen

and therefore, was within the surface ply (assuming each ply has about 20 fibers through its thickness). This portion of the fracture surface was perpendicular to the lower specimen surface in all tests. All six photomicrographs in figure 11 show some smooth fiber surfaces, indicating fiber-matrix interface failures. These photomicrographs also show matrix fracture hackles between the fibers. However, the hackles are smaller and less extensive for fiber angles in the 90° to 45° range, probably due to the previously mentioned σ_{22} dominance in this range. For smaller fiber angles, the hackles are larger and more wide spread, agreeing with hackling trends for mixed-mode delamination [12]. Because no attempt was made to precisely locate the cracking initiation site, the photomicrographs in figure 11 probably correspond to crack propagation and, therefore, should be expected to agree with delamination observations. Although all specimens in this study failed abruptly without any noticeable indication of stable damage progression, future research on this test should involve NDE procedures to detect the onset of cracking and to determine its location. Such information is needed to better understand the crack initiation mechanisms associated with ply strength under multiaxial stress states. These mechanisms may be quite different from the crack growth mechanisms associated with crack toughness. Such insight could lead to materials with higher ply strength.

CONCLUDING REMARKS

An off-axis flexure (OAF) specimen, apparatus, and test procedure have been presented to measure ply strength (cracking resistance) under multiaxial stress states. This test uses a three-point bending fixture with rotatable supports to avoid twist-induced torsion. The test specimen was evaluated using a 3D finite element stress analysis. The OAF test was then

demonstrated using graphite/epoxy specimens cut from a 24-ply unidirectional laminate using various off-axis angles to produce a range of stress states. The test results were presented and discussed in terms of the normal stress σ_{22} and shear stress σ_{12} on the fracture plane.

The stress analysis verified that the ball-bearing supports prevented undesirable torque loading and thereby allowed simple bending loads to be applied to off-axis specimens. As a result, the specimen failure stresses were calculated using simple beam theory.

The OAF tests and the data analysis procedures produced ply strength data for σ_{22}/σ_{12} ratios ranging from ∞ to 0.27. This range included stress states that were shown to be typical of ply stresses in structural laminates. This test may, therefore, prove to be useful in generating data needed to predict ply crack initiation in composite structures. The OAF test may also provide an approach for studying fiber-matrix interface treatments, using stress states that represent conditions in structures.

The off-axis flexure test introduced in this paper is believed to offer advantages over current ply strength tests and fiber-matrix interface tests. If so, this test may eventually lead to improved ply cracking predictions and, perhaps, to improved materials.

REFERENCES

[1] Pipes, R. B., "On the Off-Axis Strength Test for Anisotropic Materials," Journal of Composite Materials, vol. 7, April 1973, pp. 246-256.

[2] Sinclair, J. H. and Chamis, C. C., "Fracture Modes in Off-Axis Fiber Composites," Polymer Composites, vol. 2, Jan. 1981, pp. 45-52.

[3] Pagano, N. J. and Halpin, J. C., "Influence of End Constraints in the Testing of Anisotropic Bodies," Journal of Composite Materials, vol. II, no. 1, 1968, p 68.

[4] Rizzo, R. R., "More on the Influence of End Constraints on Off-Axis Tensile Tests," Journal of Composite Materials, vol. 3, April 1969, pp. 202-219.

[6] Cron, S. M., Palazotto, A. N., and Sandu, R. S., "The Improvement of End-Boundary Conditions for Off-Axis Tension Specimen Use," Experimental Mechanics, March 1988, pp. 14-19.

[7] Sun C. T. and Berreth, S. P., "A New End Tab Design for Off-Axis Tension Test of Composite Materials," Journal of Composite Materials, vol. 22, August 1988, pp 766-779.

[8] Swanson, S. R., Messick, M. J., and Tian, Z., "Failure of Carbon/Epoxy Lamina under Combined Stress," Journal of Composite Materials, vol. 21, July 1987, pp. 619-630.

[9] Guess, T. R. and Haizlip, C. B., Jr., "End-Grip Configurations for Axial Loading of Composite Tubes," Experimental Mechanics, Jan. 1980, pp. 31-36.

[10] Groves, S. E., Sanchez, R. J., and Feng, W. W., "Multiaxial Failure Characterization of Composites," Proceedings of the Eighth International Conference on Composite Materials, Honolulu, July 15-19, 1991, pp 37B3-37B15.

[11] Hercules Prepreg Tape Materials Characterization Data Package, Hercules Inc., Magma, Utah, Feb. 1989.

[12] Reeder, J. R., "An Evaluation of Mixed-Mode Delamination Failure Criteria," NASA TM-104210, Feb. 1992.

[13] Adams, D. F., King, T. R., and Blackketter, D. M., "Evaluation of the Transverse Flexure Test Method for Composite Materials," Composites Science and Technology, vol. 39, 1990, pp. 341-353.

Table 1.- Results from OAF tests.

α (deg)	d[a] (mm)	σ_{22} (MPa)	Avg σ_{22} (MPa)	σ_{12} (MPa)	Avg σ_{12} (MPa)
90	2.946	65.7	82.5	0.0	0.0
	2.941	71.4		0.0	
	3.457	76.6		0.0	
	3.472	92.0		0.0	
	3.454	106.9		0.0	
75	3.472	86.7	92.5	23.2	24.8
	3.490	90.9		24.4	
	3.467	91.2		24.5	
	3.465	93.9		25.2	
	3.465	99.7		26.8	
60	3.363	57.4	80.3	33.2	46.3
	3.162	76.3		44.0	
	3.274	78.3		45.2	
	3.208	91.2		52.7	
	3.353	98.0		56.6	
45	3.419	71.6	77.4	71.6	77.4
	3.393	73.6		73.6	
	3.246	77.5		77.5	
	3.203	78.7		78.7	
	3.228	85.1		85.1	
30	3.294	54.3	60.1	94.1	104.0
	3.381	58.2		100.8	
	3.399	61.5		106.5	
	3.249	62.5		108.2	
	3.312	63.6		110.3	
15	3.188	34.6	36.1	129.1	134.8
	3.211	36.1		134.7	
	2.951	36.3		135.7	
	3.175	36.8		137.5	
	3.175	38.0		141.6	

a- measured at specimen midspan.

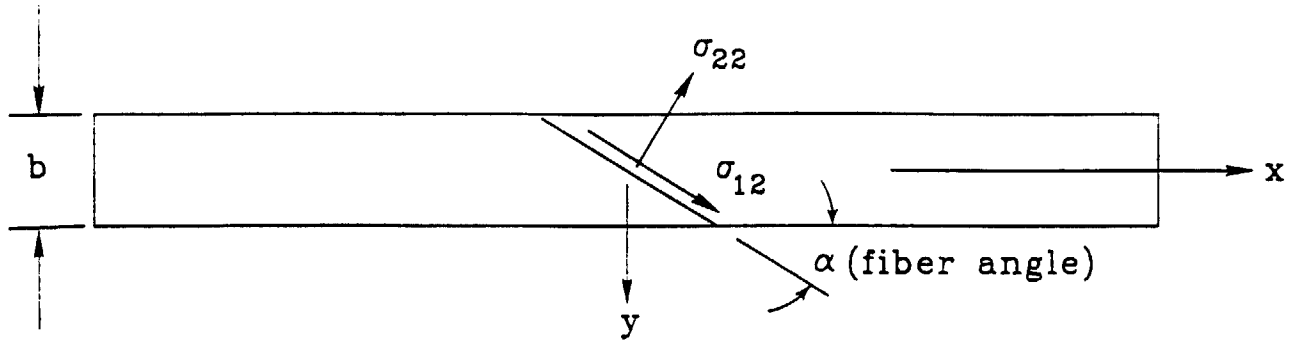

(a) Plan view of specimen.

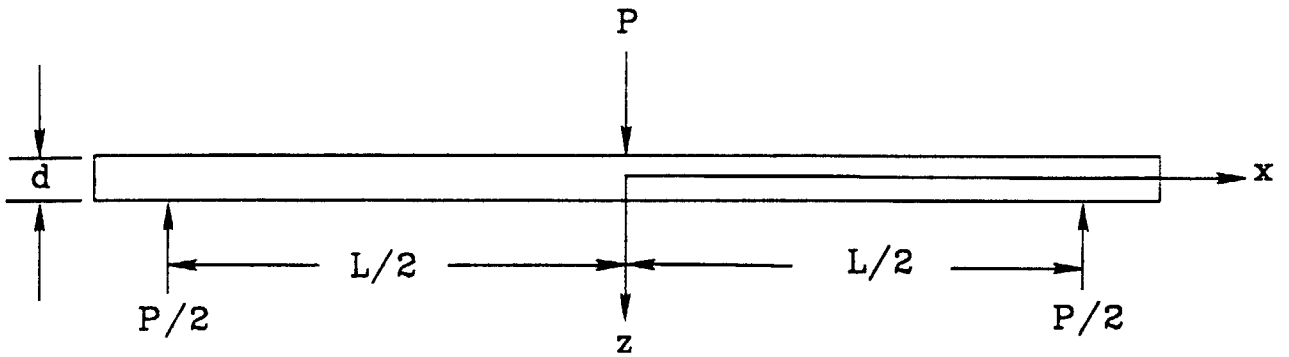

(b) Edge view of specimen with three-point loading.

Figure 1.- The off-axis flexure specimen configuration and loading.

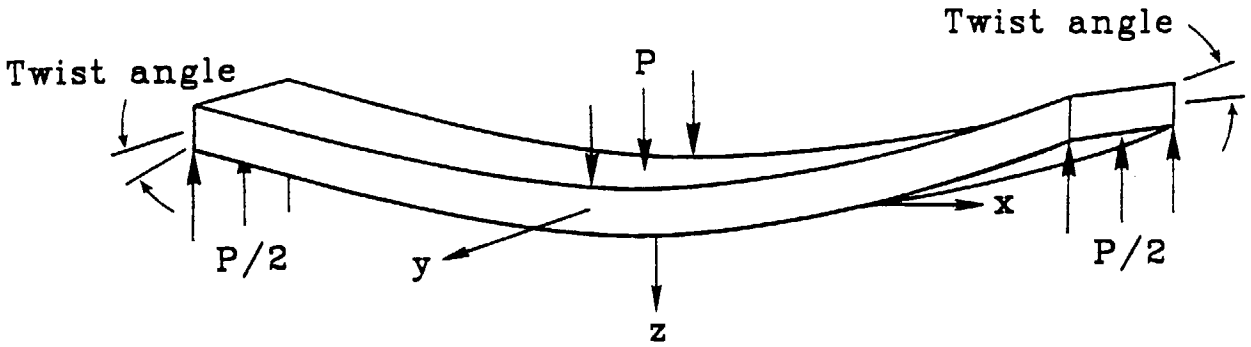

(a) Flexure and twist deformation.

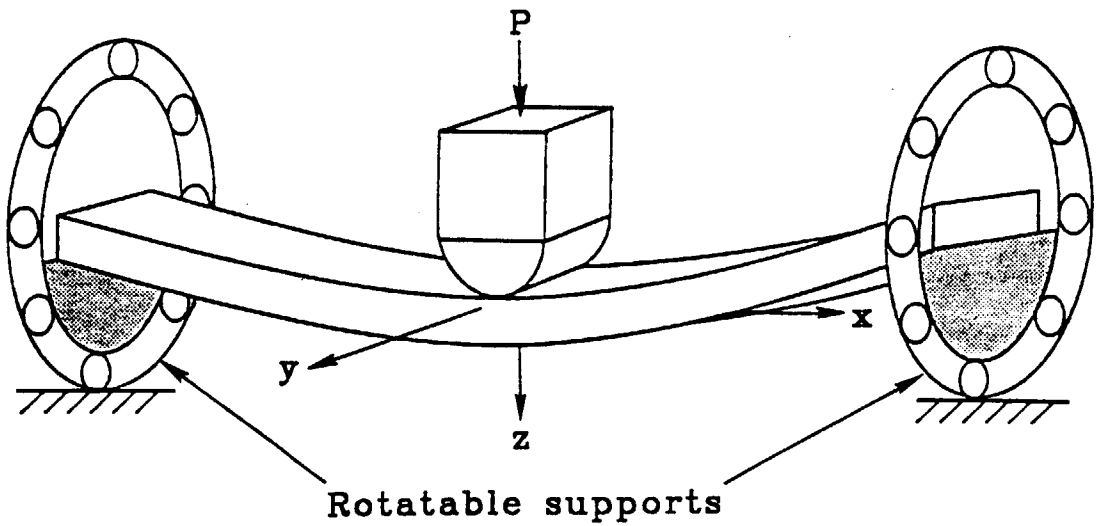

(b) Schematic of off-axis flexure test apparatus.

Figure 2.- Schematic of specimen deformation and test apparatus.

Figure 3.- Photograph of off-axis flexure test apparatus.

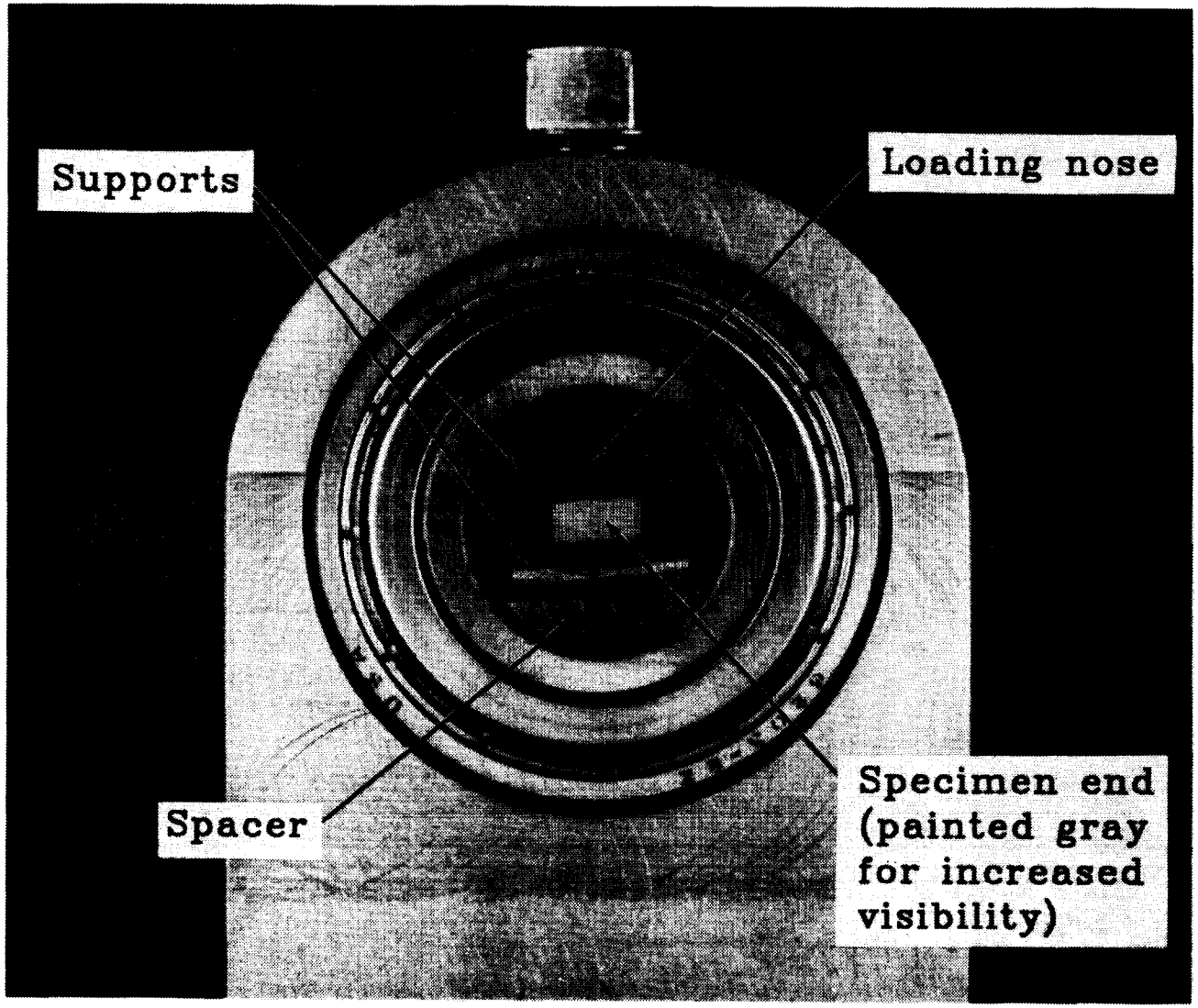

Figure 4.- End view of apparatus and deformed specimen.

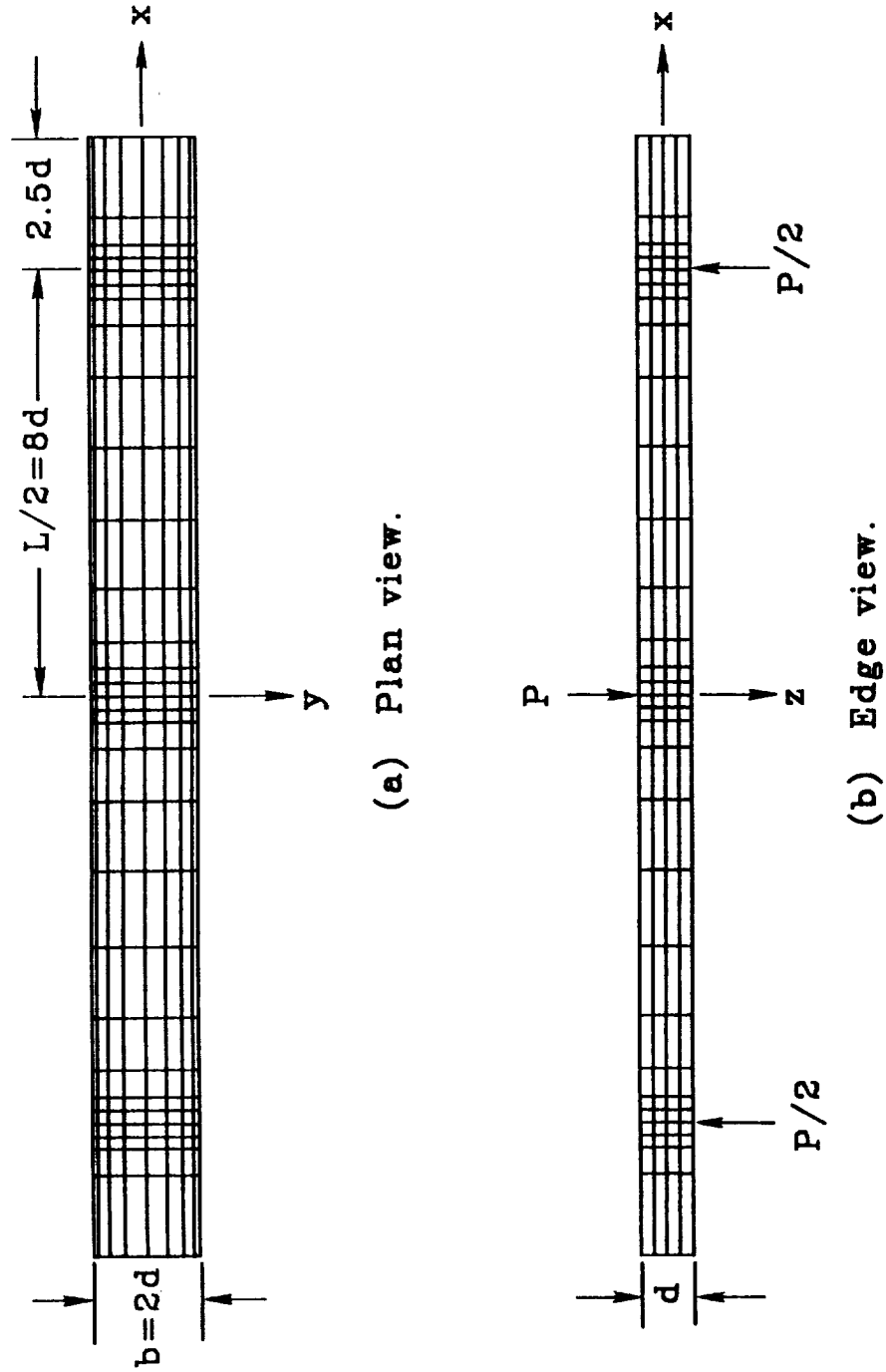

Figure 5.- Finite element model of off-axis flexure specimen.

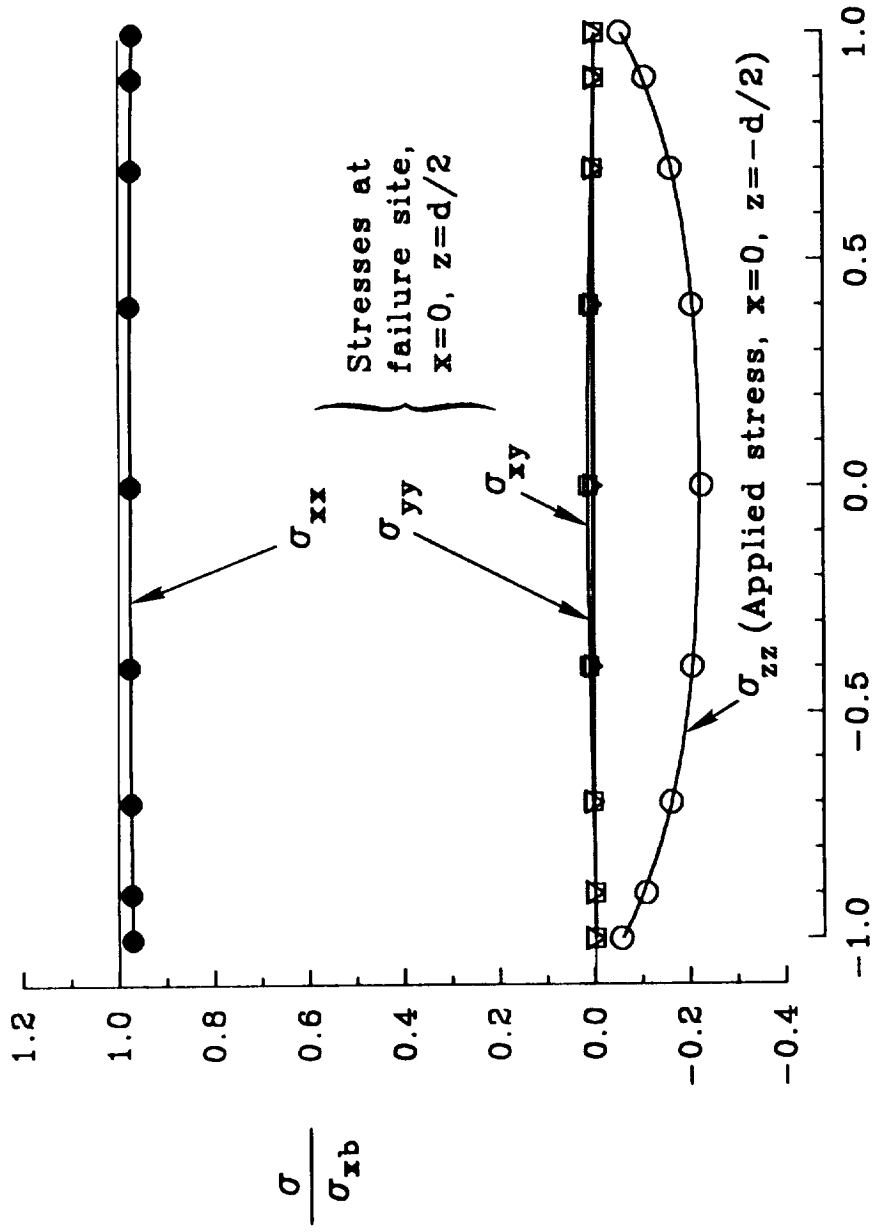

Figure 6.- Stress distributions for the 75° OAF specimen.

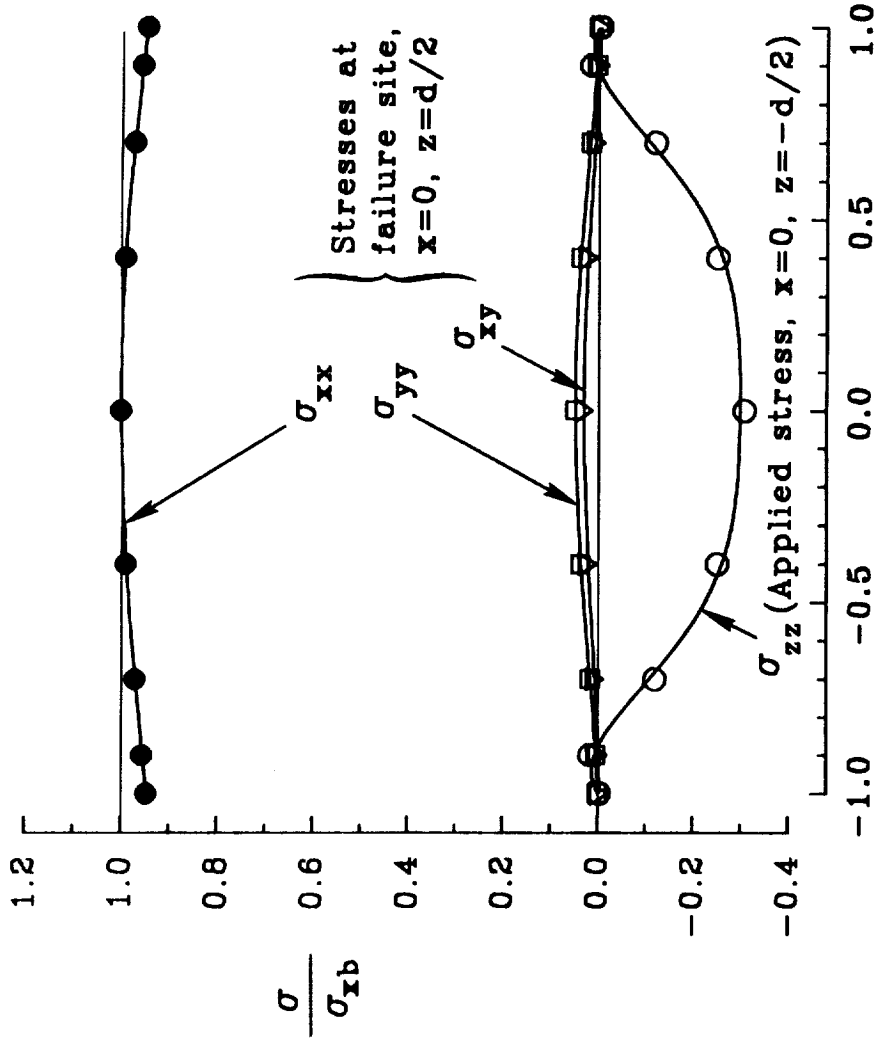

Figure 7.- Stress distributions for the 45° OAF specimen.

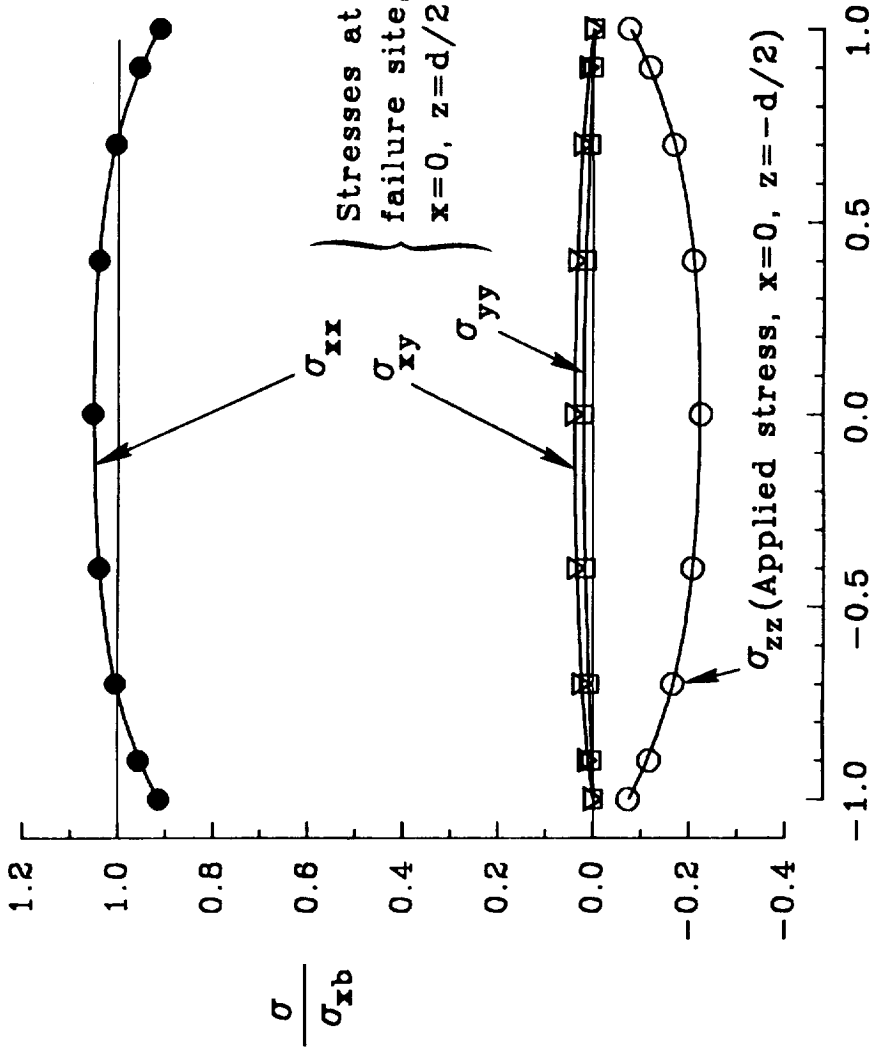

Figure 8.- Stress distributions for the 15° OAF specimen.

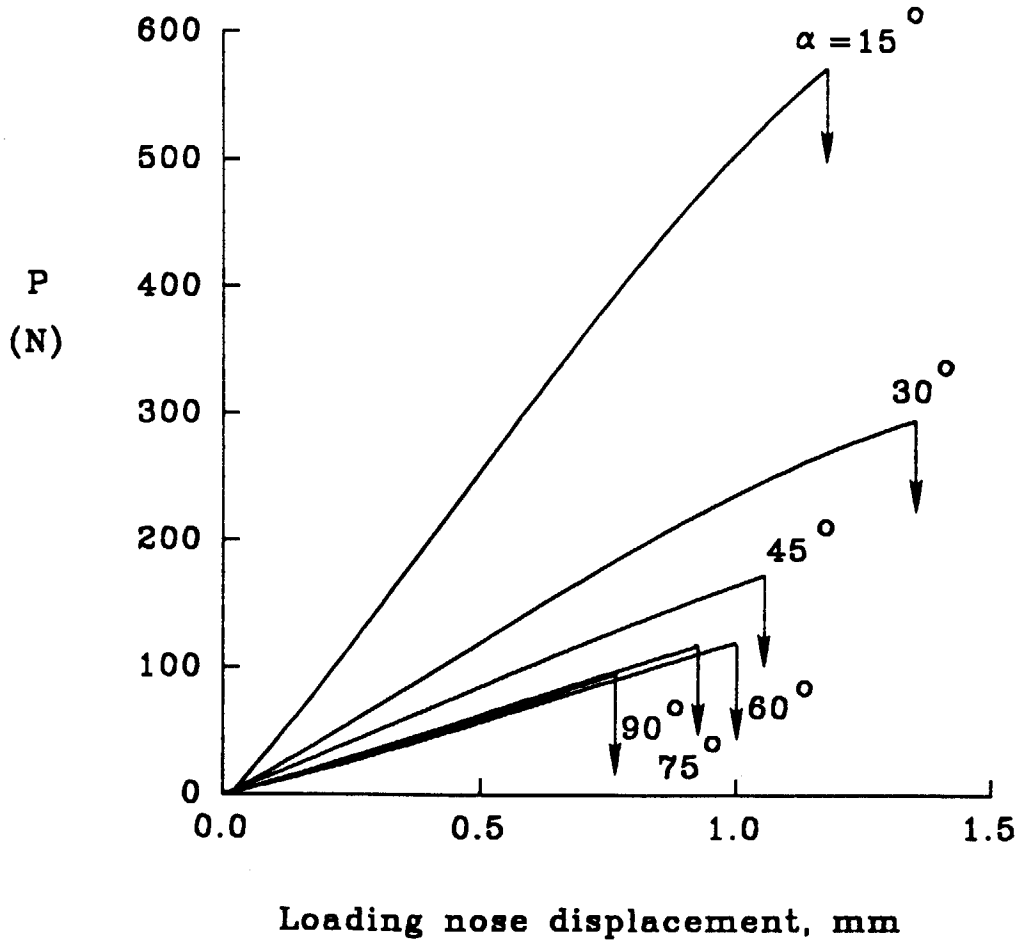

Figure 9.- Typical load displacement curves.

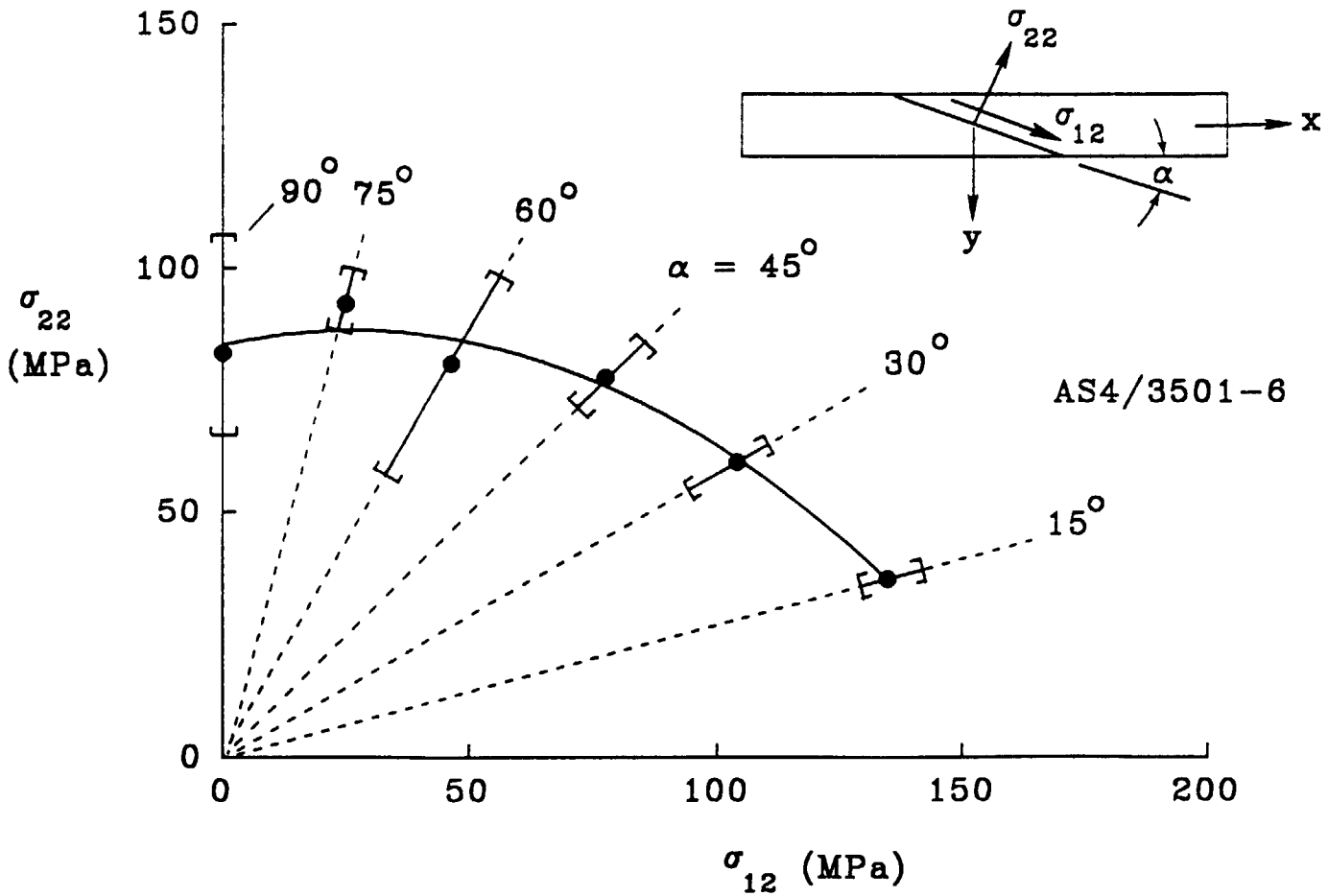

Figure 10.- Results from OAF tests with AS4/3501-6 graphite/epoxy.

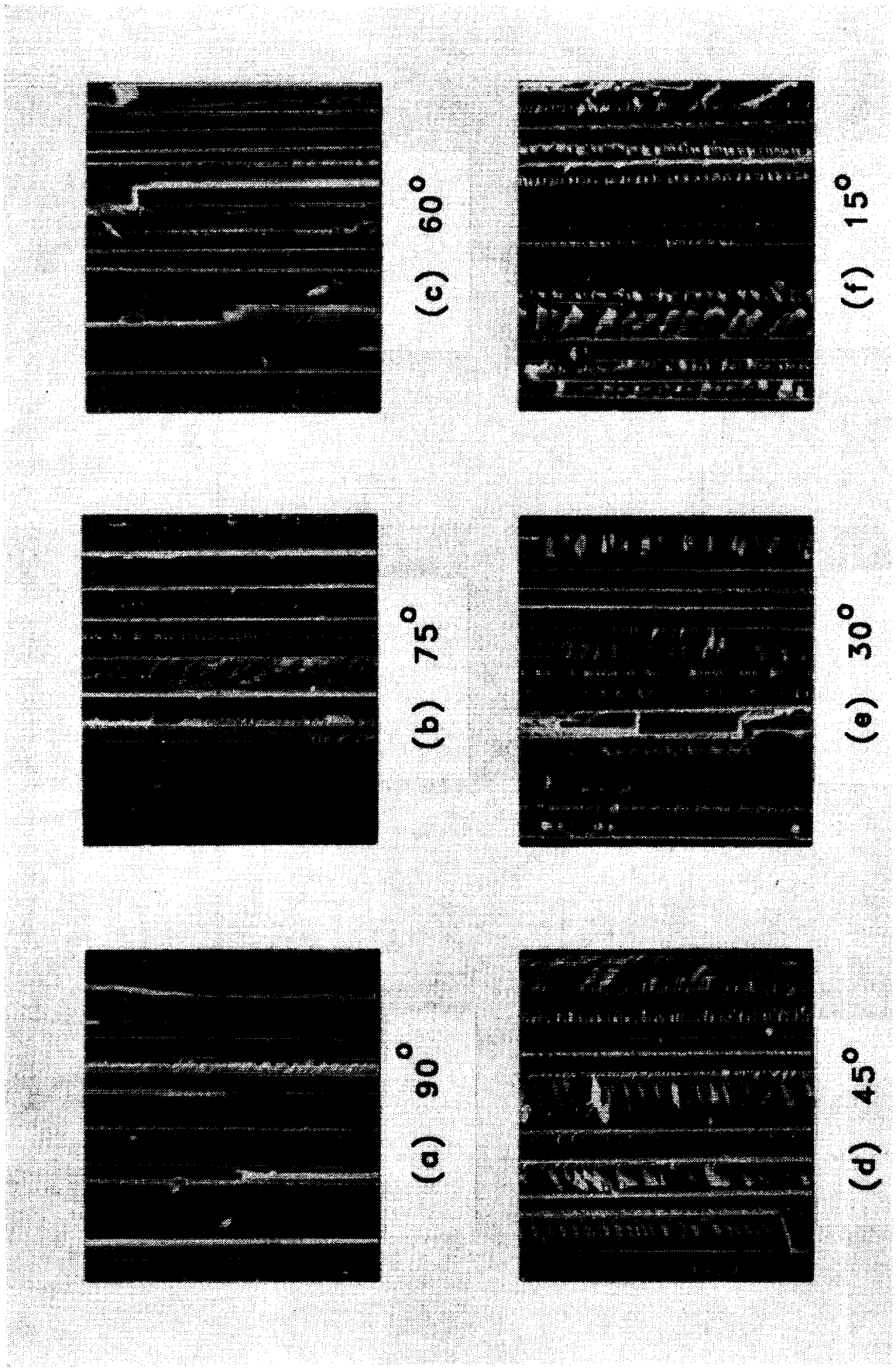

Figure 11.- Photomicrographs of OAF fracture surfaces.

REPORT DOCUMENTATION PAGE

Form Approved
OMB No. 0704-0188

1. AGENCY USE ONLY (Leave blank)	2. REPORT DATE	3. REPORT TYPE AND DATES COVERED
	March 1992	Technical Memorandum

4. TITLE AND SUBTITLE

Measurement of Multiaxial Ply Strength by an Off-Axis Flexure Test

5. FUNDING NUMBERS

WU-505-63-50

6. AUTHOR(S)

John H. Crews, Jr. and Rajiv A. Naik

7. PERFORMING ORGANIZATION NAME(S) AND ADDRESS(ES)

NASA Langley Research Center
Hampton, VA 23665-5225

8. PERFORMING ORGANIZATION REPORT NUMBER

9. SPONSORING / MONITORING AGENCY NAME(S) AND ADDRESS(ES)

National Aeronautics and Space Administration
Washington, DC 20546

10. SPONSORING / MONITORING AGENCY REPORT NUMBER

NASA TM-107570

11. SUPPLEMENTARY NOTES

Crews: Langley Research Center, Hampton, VA; Naik: Analytical Services and Materials, Inc., Hampton, VA

12a. DISTRIBUTION / AVAILABILITY STATEMENT

Unclassified - Unlimited

Subject Category 39

12b. DISTRIBUTION CODE

13. ABSTRACT *(Maximum 200 words)*

An off-axis flexure (OAF) test has been presented to measure ply strength under multiaxial stress states. This test involves unidirectional off-axis specimens loaded in bending, using an apparatus that allows these anisotropic specimens to twist as well as flex without the complications of a resisting torque. A 3D finite element stress analysis verified that simple beam theory could be used to compute the specimen bending stresses at failure. Unidirectional graphite/epoxy specimens with fiber angles ranging from 90° to 15° have combined normal and shear stresses on their failure planes that are typical of 45° plies in structural laminates. Tests for a range of stress states with AS4/3501-6 specimens showed that both normal and shear stresses on the failure plane influenced cracking resistance. This OAF test may prove to be useful for generating data needed to predict ply cracking in composite structures and may also provide an approach for studying fiber-matrix interface failures under stress states typical of structures.

14. SUBJECT TERMS	15. NUMBER OF PAGES
Composite; Ply strength; Test; Multiaxial; Off-axis flexure	29
	16. PRICE CODE: A03

17. SECURITY CLASSIFICATION OF REPORT	18. SECURITY CLASSIFICATION OF THIS PAGE	19. SECURITY CLASSIFICATION OF ABSTRACT	20. LIMITATION OF ABSTRACT
Unclassified	Unclassified		